Soil loss and sediment yield in a perennial catchment in southwest Piauí, Brazil

Kamylla Gonçalves Oliveira Assis · Yuri Jacques Agra Bezerra da Silva ⓘ · José Wellington Batista Lopes · João Carlos Medeiros · Marcos Paulo Rodrigues Teixeira · Fernando Braga Rimá · Vijay P. Singh

Abstract Soil and water are vital natural resources. However, due to their indiscriminate use, these resources are being seriously threatened. Therefore, it is essential to manage them in a sustainable way and leave them for future generations. Population and agricultural areas have expanded, deforesting native landscapes for cultivation and pastures. As a result, soil loss from agricultural areas is increasing the amount of sediment transport in water courses. The objective of this study was to quantify soil loss and sediment yield from the Corrente dos Matões sub-basin (CMSB). These measurements are essential to quantify the environmental impact of advancing agricultural frontiers. The Universal Soil Loss Equation (USLE) was applied due to its wide use, compatibility with GIS, and data availability. The suspended sediment transport was calculated by collecting samples with DH-48 sampler. From the application of USLE, the average soil erosion contributed very little to sediment delivery in the watercourse, with a magnitude of only 0.37 t ha^{-1} year^{-1}. The highest soil loss was associated with greater slope and was observed in areas with agriculture or under the absence of vegetation cover. The low transport of suspended sediments in CMSB is due to the existence of preserved sites. About 99% of the sub-basin had a low degree of erosion. The high degree of soil loss was attributed to the cliffs and the development of agricultural activities leaving the soil uncovered. This work will help identify the most susceptible areas to water erosion for optimizing the allocation of financial resources for the preservation of this natural resource.

Highlights Soil loss and sediment transport were measured under different scales.
About 99% of the sub-basin had a low degree of erosion.
The average annual loss of soil predicted by the USLE was 0–1 t ha^{-1}.
The high degree of soil loss was attributed to the cliffs.
The suspended sediment yield equal to 0.89 t km^{-2} year^{-1} was considered low.

K. G. O. Assis · Y. J. A. B. da Silva (✉) · J. W. B. Lopes · M. P. R. Teixeira
Agronomy Department, Federal University of Piaui (UFPI), Planalto Horizonte, Bom Jesus, PI 64900-000, Brazil
e-mail: yurijacques@ufpi.edu.br

J. C. Medeiros
Federal University of Southern Bahia (UFSB), Itabuna, BA 45604-810, Brazil

F. B. Rimá
Federal Institute of Maranhão (IFMA), Codó, MA 65400-000, Brazil

V. P. Singh
Biological and Agricultural Engineering Department, Zachry Department of Civil Engineering, Texas A&M University, College Station, TX 77843-2117, USA

Introduction

Quantification of soil loss at different scales, including plots under simulated rainfall and measurement of sediment transport and yield in river basins, is essential for proper

management of water resources. The erosive process is often intensified by the increase in agricultural areas, damaging preserved areas, which accelerate the transfer of sediments and contaminants to water courses (Minella et al. 2014; Shivhare et al. 2018; Rey 2003; Ochoa et al. 2016; Mehri et al. 2018; Tian et al. 2020). Sediments can be transported on the riverbed as bed load or in suspension as suspended load, which is often the highest contribution to sediment yield and transfer of contaminants (Silva et al. 2015, 2018; Guo et al. 2018). In addition to chemical problems, the excessive amount of sediment causes economic losses, mainly due to the sedimentation of rivers and reservoirs (Batista et al. 2017; Zhou et al. 2019; Aghsaei et al. 2020).

Soil loss can be determined using mathematical models or by direct measurements of sediment transport in watercourses. These measurements are essential to quantify the environmental impact of advancing agricultural frontiers (Júnior et al. 2019; Hao et al. 2012). The Universal Soil Loss Equation (USLE) is used for the quantification of rill and interrill erosion and allows for integration with remote sensing, geoprocessing, and modeling of environmental processes (Singh and Panda 2017; Alewell et al. 2019). Júnior et al. (2019) used USLE to assess the influence of land use change on erosion in a tropical basin.

The Corrente dos Matões sub-basin (CMSB) is the only perennial water resource in the Gurguéia watershed—the second largest watershed in the State of Piauí and an affluent of the Parnaíba River. This water resource mainly includes areas for soybean and livestock which can increase erosion and sediment yield. Despite some areas with preserved riparian vegetation, mainly close to the channel banks, sedimentation has been observed in almost the entire stream, especially downstream and close to the outlet. Therefore, the objective of this work was to quantify soil losses using simulated rainfall and USLE as well as quantify sediment transport and yield at the CMSB. Results will help identify the most susceptible areas to water erosion and optimize the allocation of financial resources for the preservation of this natural resource.

Material and methods

Studied catchment

Located in the municipality of Bom Jesus, southwestern portion of the state of Piauí (9° 01′ 52″ and 9° 20′ 00″ South and 44° 25′ 34″ and 44° 52′ 16″ West) (Fig. 1), the CMSB covers an area of 964 km^2, within a perimeter of 168.7 km in length and 63.5 km in length of the main water course.

At approximately 360 m of altitude, the CMSB is the main tributary of the Gurguéia River which empties into the Parnaíba River—the largest genuinely northeastern river being navigable in its entire length of more than 1400 km. The climate is warm and semi-arid. The average annual rainfall is 900 mm, ranging from 800 to 1200 mm. The rainiest period is from December to April. The temperature ranges from 18 to 36 °C. The predominant geomorphology in the region is the wide, flat, or slightly wavy tabular surface, limited by steep escarpments that can reach 600 m, showing relief with lowered and dissected areas. The CMSB's relief is predominantly flat. The predominant soils are Oxisol, Entisol lithic, and Entisol fluvents (Fig. 1).

In the sub-basin area, there is a well-preserved flora typical of the Cerrado forest, with the presence of semideciduous, deciduous, and epiphytic species, and of typical caatinga forest, with the presence of trees and low shrubs with twisted branches, creeping herbs, and cactus. It is also possible to verify the presence of permanent preservation area that borders the river course. The densest Cerrado vegetation and areas with agriculture and livestock cover around 33 and 27%, respectively.

Soil collection and physical and chemical analysis

Fifty-nine composite samples (0–10 cm) were collected, according to the methodology described by Teixeira et al. (2017). The organic carbon content of the samples was determined by wet digestion $K_2Cr_2O_7$-H_2SO_4 (Yuan 1963). The granulometric analysis was determined by the pipette method (Gee and Bauder 1986).

Estimation of parameters of the Universal Soil Loss Equation

The use of USLE was preceded by a survey of secondary data, determination of qualitative primary data, determination of quantitative primary data by on-site experiment, classification of orbital images, and integration of data from the analysis and processing in the environment of geographic information systems.

The methodology proposed by Bertoni and Lombardi (2005) was used to obtain the erosivity factor
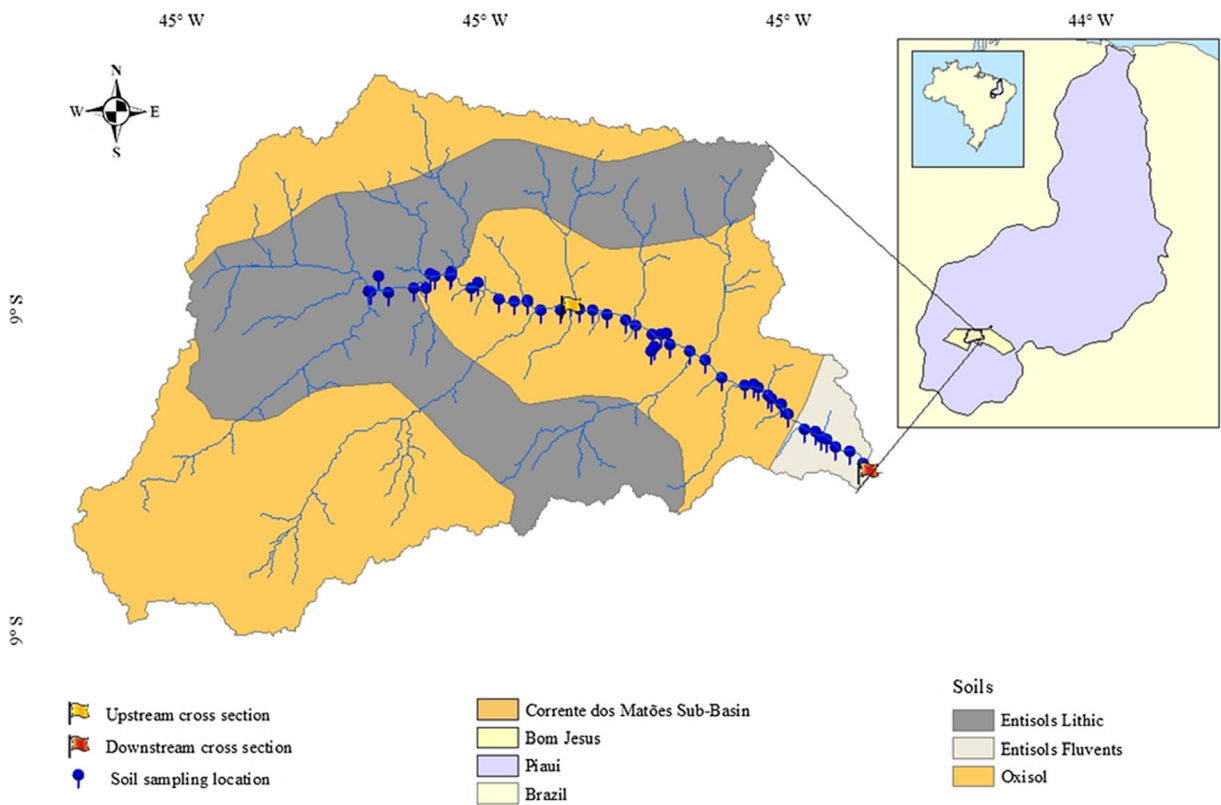
Fig. 1 Sampling sites and soil classes of the CMSB

(R). The values were interpreted according to Carvalho (1994): low ($R < 2452$), medium ($2452 < R < 4905$), medium to strong ($4905 < R < 7357$), strong ($7357 < R < 9810$), and very strong ($R > 9810$).

The erodibility factor in the area composed of Oxisols was obtained through a direct and an indirect method. In the first case, a rainfall simulator was used, and the final value compared to the estimated value obtained by the indirect method (nomogram). The experiment was carried out in experimental plots with a useful area of 0.70 m^2 delimited by galvanized steel sheets. Before the application of rain, the soil moisture standardization was carried out through micro sprinkler. The simulated rain was applied with a portable rainfall simulator model InfiAsper, developed by Alves Sobrinho et al. (2008). This equipment was calibrated before the test with a rain intensity of 65 mm h^{-1}. Each test lasted 60 min from the beginning of runoff.

The methodology described in Panachuki et al. (2011) was used to evaluate runoff in each treatment, in which the volume drained with the aid of plastic pots with a capacity of 1 l was collected. A runoff sample was collected every 2 min. After measuring the runoff

volume, every 6 min a sample was stored, totaling 10 samples for each treatment. The sediment mass was obtained by the evaporation method. From these values, soil loss and erodibility were calculated. To estimate soil erodibility values, an indirect method proposed by Wischmeier (1978) was used. To facilitate the work, an approximation of the nomogram, developed by Arnold (1994), was used.

The topographic factor (LS) was elaborated from data obtained from the Digital Elevation Model (DEM) provided by NASA's Shuttle Radar Topography Mission (SRTM). The equation proposed by Bertoni and Lombardi (2005) (Table 1) was also used by Corrêa and Dedecek (2009). To finalize the LS map, it was necessary to individually obtain the slope length (λ) for each pixel in the DEM.

E_L, soil loss; R_{ij}, rainfall erosivity; K_i, soil erodibility, LS_i, topographic factor, CP_{ij}, soil cover and conservation practices, Pm, average monthly total rainfall (mm); Pa, average annual total rainfall (mm). Ka, % of organic matter; Kb, coefficient relative to the soil structure ($b = 1$ for very fine granular structure; $b = 2$ for fine granular structure; $b = 3$ for medium or coarse granular structure;

Table 1 Description of parameters of the universal soil loss equation

Variable	Equation	Unit
E_L	$R_{i,j}.K_i.LS_i.CP_{i,j}$	t ha^{-1}
Rj	$67.3550*(Pm^2/Pa)^{0.85}$	MJ mm ha$^-$1 h^{-1}
K_i	$(2.1 \times 10^{-4}*M^{1.14}**(12-ka) + 3.25(kb-2) + 2.5(kc-3))*0.001317$	t ha^{-1}/MJ ha^{-1} mm h^{-1}
M	(% silt + fine sand) × (100 − % clay)	%
LS_i	$0.00984 \times \lambda^{0.63} \times D^{1.18}$	Pixel
λ		Pixel
	$\sqrt{Px^2 + \left[\left(\frac{S}{100}\right) \times Px\right]^2}$	

$b = 4$ for block, laminar or massive structure); Kc, permeability class ($c = 1$ for fast permeability; $c = 2$ for moderate to fast permeability; $c = 3$ for moderate permeability; $c = 4$ for slow to moderate permeability; $c = 5$ for slow permeability; $c = 6$ for very slow permeability). Px, pixel size; and S: land slope

In order to verify possible changes in the landscape along the main water course that influence the C and P factors of USLE, trips were made and divided into six phases: three in each semester of the year. The degree of conservation of the vegetation filter strips and permanent preservation sites was evaluated, based on a qualitative model, for assessing the characteristics and level of environmental impacts resulting from human activities and the conditions of habitat and level of conservation. The evaluation of model was used during the visits and monitoring, allowing changes in the area to be monitored. The representative aspects at each point were noted, recorded with a camera with a remotely piloted aircraft (RPA) of the quadricopter type. Each point was also geolocated with a navigation GNSS receiver. In this model, the presence and appearance of water, forms of land use, and conservation status of vegetation and soil were considered.

Finally, the C factor was obtained with the aid of a Landsat satellite image 8 ETM sensors from October 21, 2017, from orbit and point 220/66. The image classification was performed using the compositions to express plant and soil components (i.e., vegetation (comp_654) and combination to differentiate water from soil, highlighting vegetation (comp_564) and bands 4, 3, and 2 which corresponded to the infrared, red, and green bands of the spectrum, respectively). This image was classified using the classification method supervised by the maximum likelihood algorithm. Subsequently, four classes were defined within the basin: water, thin

vegetation, dense vegetation, and bare soil. Once the image of area was classified, the percentage of each class was calculated, and the corresponding value of the C factor recommended by Fujihara (2002) was determined, which determined the factor C as 0, 0.01, 0.025, and 1 for water, dense vegetation, thin vegetation, and bare soil, respectively.

At the end, the map of soil loss was made from the interaction of each USLE factor, being possible to generate the following maps: erosivity, erodibility, topography, and land use. These databases were integrated by map algebra, where the maps of each factor necessary for the application of USLE were used: the LS factor that constitutes the effect of slope and the C and P factors considered in the vegetation cover map, factor K, and factor R. By combining these maps, it is possible to categorize the territory and obtain a map of homogeneous units susceptible to erosion. The results were classified according to Pham et al. (2018) (t ha^{-1}): very low erosion (0–1), low erosion (1–5), medium erosion (5–10), high erosion (10–50), and extreme erosion (> 50).

Hydraulic flow characterization and sediment yield

CMSB's hydrosedimentometric monitoring was carried out in two cross sections located upstream and downstream of the main watercourse. The upstream cross-section presented the mean values for the width and height of the water flow equal to 6.2 m and 0.42 m, respectively; for the downstream section, the values were 4.7 m and 0.6 m, respectively. The average flow velocity (m s^{-1}) was obtained during the period of low and high flow regime using a current meter. The number of points on which the windloss was positioned varied according to the water flow depth at the time of each

measurement (Back 2006). The flow was calculated by the product between the cross-sectional area and the average flow velocity (Table 2).

Q_l water discharge (m^3 s^{-1}); Q_i, water discharge of each profile (m^3 s^{-1}); A_i, area of influence of each vertical (m^2); V_i, average flow velocity in each vertical (m s^{-1}). V, flow velocity (m s^{-1}); K, proportionality constant (i.e., 0.4 for the sampler tip ¼"); $T_{sampling}$, minimum time for sampling (s); h, depth of the sampling vertical (m); V_t, transit ratio (m s^{-1}); C_{ss}, suspended sediment concentration of each vertical (mg L^{-1}); M_{sed}, mass of the sediment (mg); V_{sample}, sample volume (L); Q_{ss}, suspended sediment discharge (t day^{-1}); Q_l, net discharge from the respective vertical (m^3 s^{-1}). P_s, sediment yield (t day^{-1}); A, sub-basin area (Km^2); R_e, Reynolds number (dimensionless); R_h, hydraulic radius (m); v, kinematic viscosity of water; F_r, Froude number (dimensionless)

The sampling of suspended sediment was carried out according to the Equal Width Increase (IIL) method (Edwards and Glysson 1999). The suspended sediment was collected using the US DH-48 sampler. This equipment is one of the most suitable ones for the flow characteristics of the sub-basin and allows for obtaining isokinetic samples. The transit ratio was calculated from the adjustment proposed by Edwards and Glysson (1999). This minimum sampling time was calculated according to Carvalho et al. (2000) and Merten and Poleto (2006). The sediment mass was obtained following the evaporation methodology (USGS 1973). The suspended sediment concentration (SSC) for each vertical was calculated by the ratio between the mass of dry sediment and the sample volume. With the data of suspended sediment concentration, it was possible to

Table 2 Description of sediment transport variables in CMSB

Variable	Equation	Unit
Q_l	$\sum_{i=i}^{n} Q_i = \sum_{i=1}^{n} A_i \times V_i$	m^3 s^{-1}
V_t	$V_e \times K$	m s^{-1}
$T_{sampling}$	$\frac{2h}{V_t}$	s
SSC	M_{sed}/V_{sample}	mg L^{-1}
QSS	$\sum(SSC_i \times Ql_i) \times 0.0864$	t day^{-1}
P_s	$Qss \times 365/A$	t day^{-1}
R_e	$V \times Rh/v$	Dimensionless
F_r	$V/\sqrt{(9.8*Rh)}$	Dimensionless

calculate the Coefficient Box that defines the sampling accuracy.

The suspended solid discharge was determined by the sum of the product between the CSS and the respective Q. The sediment yield was calculated by the average of the product of the suspended solid discharge and the total area of the basin.

Results and discussion

Measuring soil erosion and obtaining USLE parameters

The average soil loss in the experimental plots submitted to simulated rainfall in Oxisols was equal to 0.001321 t ha^{-1}. This value was considered low according to Pham et al. (2018). The texture of the sandy loam soil provided greater water infiltration to the detriment of runoff and, therefore, a reduced and low energy liquid discharge for the displacement of solid material. In field conditions, the low value of soil loss in Yellow Latosol was attributed to soil preparation at a level, providing unfavorable conditions to the increase in runoff and, consequently, the soil loss (Kok and Kim 2019). Another factor is the soil texture, sandy loam, which provided greater water infiltration to the detriment of runoff.

The average value of rainfall in the CMSB was 912 mm year^{-1}. These values were similar to those presented by Andrade Júnior et al. (2004), who identified an average annual rainfall of 800 to 1000 mm for the southern region of the state of Piauí. The R factor obtained through the methodology proposed by Bertoni and Lombardi (2005) was 6348 MJ mm ha^{-1} year^{-1} (Fig. 2a). Close values were found by Morais and Sales (2017) in the same region (6256 to 6319 MJ mm ha^{-1} year^{-1}). Based on the classification proposed by Carvalho (1994), the CMSB erosivity was considered medium to strong and, therefore, agricultural practices that promote soil detachment, changing the surface conditions of the land, should be used carefully, especially from November to March.

The spatial distribution and the magnitude of erodibility factor (K) varied between 0.0593 and 0.0382 t h MJ^{-1} mm^{-1} (Fig. 2b). Low values represent more resistance of the soil to the detachment by high intensity rains. The Entisol lithic showed greater erodibility due to the lower contents of organic matter and clay. According to Brady and Weil (2009), soil erodibility is
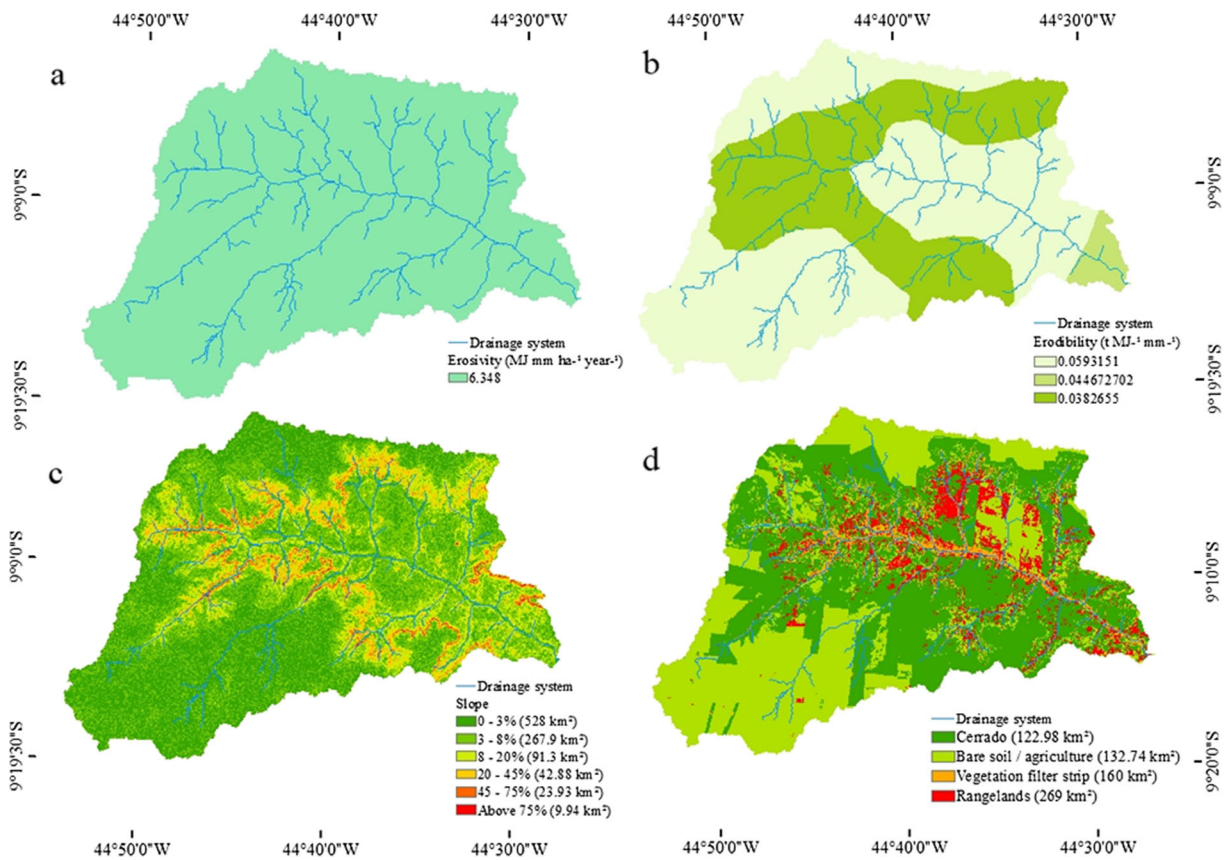
Fig. 2 Maps of erosivity (**a**), erodibility (**b**), slope (**c**), and land use (**d**) of CMSB

influenced, above all, by the infiltration capacity and structural stability.

A considerable part of the sub-basin showed the K values greater than 0.05 t h MJ^{-1} mm^{-1}, indicating a high susceptibility to water erosion. The erodibility of the Oxisol, calculated by direct and indirect methods, presented practically similar values, 0.0593 and 0.0534 t MJ^{-1} mm^{-1}, respectively, increasing the reliability of results.

The CMSB has a predominantly flat and smooth wavy relief, covering about 54% and 27% of the sub-basin area, respectively (Fig. 2c). The flat relief areas are mainly located at the top of the plateaus, as well as along the river plain, while the smooth wavy relief extends throughout the territory of the sub-basin, as well as the wavy relief that occurs in 10% of the sub-basin area (Fig. 2). The areas of strong wavy and mountainous relief (4% and 2% of the basin, respectively) occur especially at the headwaters of drainage and at the base of the exhausts of the plateaus. The areas of strong mountainous relief (1% of the sub-basin) are associated with the escarpments eroded at the edges of the plateaus and plateaus.

Analysis of the topographic factor is important in the application of USLE, since this parameter characterizes the speed of runoff and, therefore, is an indicator of the risk of soil erosion in watersheds. In the field of soil management, it is important to determine whether areas with higher LS values coincide with areas of greater erodibility and low soil coverage (high soil exposure) to identify the areas at greatest risk to water erosion and where conservation needs to be intensified.

It is worth noting that the escarpments eroded at the edges of plateaus, common and naturally occurring in productive cerrado areas, limit the applicability of erosion models based on USLE when applied spatially. These interfere when determining the contribution or effective influence of the parameters related to slope and slope length, limiting the modeling and tending to overestimate and generate erosion peaks outside the average representativeness of the area. In these bands of abrupt topography change, it is necessary to carefully parameterize the slope and length factors of the USLE or even to exclude these bands.

The southwestern part of Piauí, where CMSB is located, is in a growing development of agribusiness. The area where the grains are grown spends most of the year in the absence of vegetation cover. About 38.02% of the area is reserved for agriculture and 8.32% under pasture (Fig. 2d). The intensification of monoculture and pasture cultivation can offer efficient vegetation cover to the soil, accelerating erosion processes.

Soil loss

The estimated soil loss for CMSB ranged from 0.01 to 76.64 t ha^{-1} year^{-1}. The results clearly indicated that the average soil erosion of CMSB contributed little to the delivery of sediments in the watercourse and had a magnitude of only 0.37 t ha^{-1} year^{-1}. The results showed that 99% of the total area of the study was under the low rate of soil loss (i.e., < 5 t ha^{-1} year^{-1}) which seemed to be tolerable according to the established limits, especially for the flatter areas (Fig. 3). The area in which the soil rate was greater than 10 t ha^{-1} year^{-1} occupied less than 1% of the total area, mainly in high slopes. This area was mainly affected by the high to extremely high rate of soil loss through erosion. These values were concentrated in areas where the slope was relatively high and the undulating topography was combined with little or no soil cover.

These results allowed for the hypothesis that there was a compensatory effect of attenuating vegetation on the sedimentological processes in the basin to the point that there was a break in the connectivity of sediments from agricultural areas and eroded escarpments, making it impossible for these materials to reach the channel (Okin et al. 2015; Saco et al. 2020). In this way, the degree of connection between the sediment detachment sites and the drainage network was minimized due to the accelerated dissipation of the transfer of energy and matter between two topographic units. Understanding the dynamics about the connectivity patterns in the basin allowed the efficient targeting of practices to control the processes of erosion, sedimentation, and sediment transport, being able to guarantee the water quality, due to the
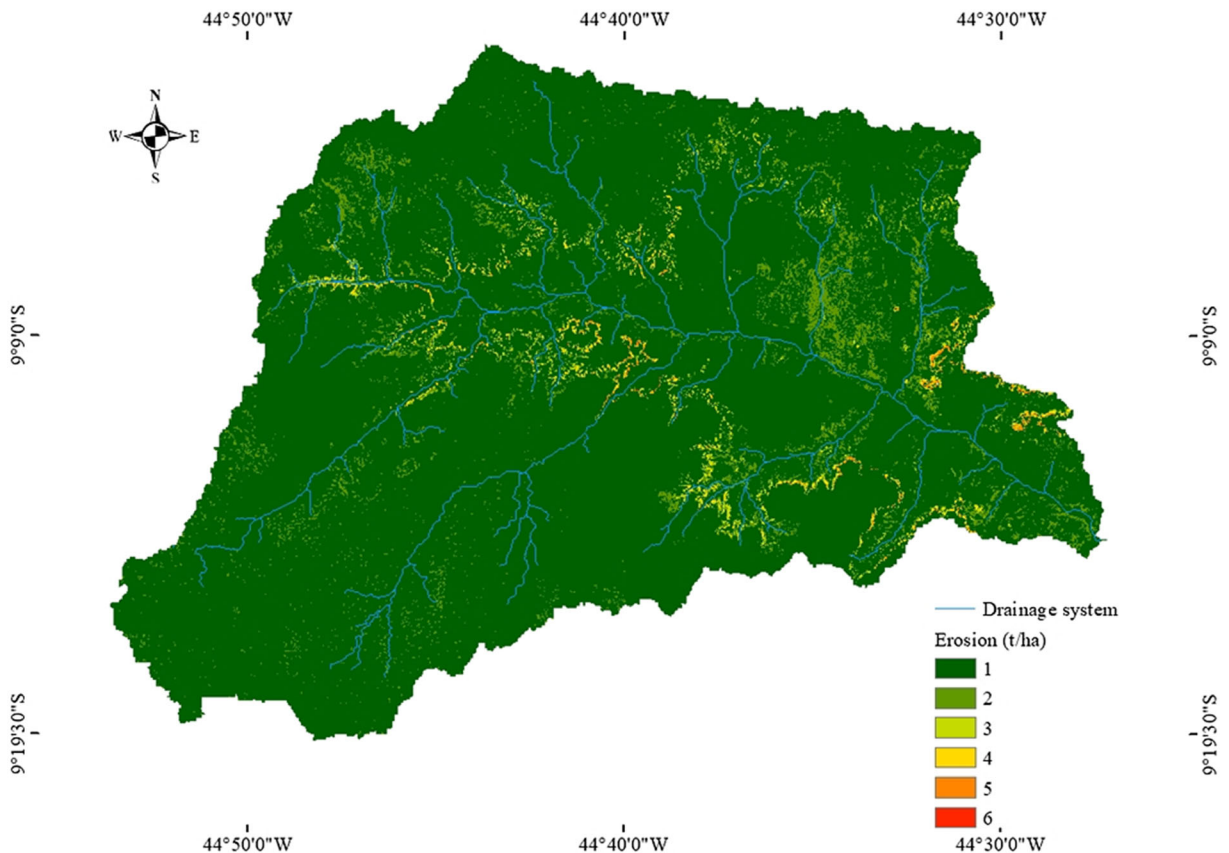

Fig. 3 Soil erosion map in CMSB

reduction of eutrophication by the increase in the quantity of nutrients; and soil fertility, due to less soil loss.

In order to maintain the current trend of soil erosion and minimize the high rate of erosion in some parts of the area currently observed, some means of conservation need to be implemented on a priority basis, which will help prevent erosion from other areas. According to Ali and Hagos (2016), high values of soil loss result from the combination of steep slopes, high rainfall, and soils with little or no vegetation cover due to anthropic influences such as deforestation and activities such as livestock, located in the areas most sensitive to erosion. According to El Jazouli et al. (2019), any decrease in vegetation cover will have a direct consequence on the rate of soil erosion. In addition, deforestation in soil areas is one of the most relevant factors in erosion induced by the change in land use. Panagos et al. (2015) observed that factor C and its associated rates of soil loss can potentially be influenced by changes in land use, especially deforestation.

Validation is one of the main challenges with erosion models, and it can be carried out by surveying and simulating soil loss (Lazzari et al. 2015; Ganasri and Ramesh 2016). However, there are always difficulties due to the scarcity of measured data to correlate the results of the simulated model. SBRCM is located in the countryside and has problems with the distribution of energy and water. In the area of Oxisols, it was possible to compare the erodibility values obtained in the field directly with the estimated values. The values were practically identical, confirming the reliability of prediction.

It was observed that only 1% of the sub-basin was classified as high and extreme erosion classes. However, there were indications that soil erosion in the study area would increase due to the use of more areas for the cultivation of annual crops and pasture and under land use and management systems that did not apply soil conservation practices properly. Other studies reinforced intensive agriculture as an adverse factor to soil conservation (García-Ruiz et al. 2013; Nunes et al. 2011; Gessesse et al. 2015). This expansion can lead to an increase in soil loss rates, increasing the supply of sediments to drainage channels, solubilization, and leaching of phosphate fertilizers (NPK). In addition, the intense mobilization of agricultural land can favor the silting and eutrophication of reservoirs, as discussed by Pantano et al. (2016). For this reason, CMSB requires attention to areas classified as medium to extreme in terms of soil conservation.

Sediment transport

In the upstream cross section, it was found that the lowest concentration of suspended sediments (7.73 mg L^{-1}) occurred in the non-rainy period and under a flow rate of 0.10 m^3 s^{-1}. The highest suspended sediment concentration was 136.61 mg L^{-1}, with a flow rate of 0.17 m^3 s^{-1}. The Reynolds and Froud numbers ranged from 18126.22 to 30247.41 and from 0.04 to 0.05, showing greater turbulence associated with flow during the high flow period. In the downstream section, the lowest concentration of suspended sediments (6.41 mg L^{-1}) was found in the non-rainy season with the flow rate of 0.24 m^3 s^{-1} and the highest concentration (99.28 mg L^{-1}) in the rainy season, with a flow rate of 0.31 m^3 s^{-1} (Table 3). The Reynolds and Froud numbers ranged from 54765.53 to 63569.1 and from 0.04 to 0.07, respectively, demonstrating greater energy associated with downstream flow, as reinforced by the higher mean value of suspended sediment discharge.

The greatest variations in the suspended sediment concentration were triggered by the high variations in rainfall events, which coincided with the high variation in the transport of suspended sediments (Table 3). The largest transport of suspended sediments occurred in the downstream cross section due to the higher values of flow and turbulence associated with flow (Table 3). This result indicated that not only runoff played a relevant role in the movement of soil particles, but also that the process of soil erosion was still substantially affected by other factors, including erodibility, slope, use, and management of the soil.

Some local conditions may justify an increase in sediment from one section to another. The first visible aspect was the contribution of sediments from crops. The cross section located upstream was close to the preserved areas, in a sparsely populated area; the second monitoring section was located near the mouth of the stream, where there was a contribution of sediment from cattle farms and crops. However, the suspended sediment yield equal to 0.89 t km^{-2} $year^{-1}$ was considered low.

All these characteristics are especially important, since during the dry season the soils in the Cerrado region are not normally cultivated, making the surface even more exposed to rain. With the use of USLE, it was possible to estimate soil loss per year, but not all of this eroded soil reached CMSB directly, as can be seen through direct measurement campaigns for suspended

Table 3 Variables for sediment transport in the upstream and downstream cross sections

Measurements	P (mm)	CSS (mg L^{-1})	CB	QSS (t day^{-1})	Q (m^3 s^{-1})	CSS (mg L^{-1})	CB	QSS (t day^{-1})	Q (m^3 s^{-1})
		Upstream				Downstream			
03/10/2018	0	7.73	0.1	0.08	0.1	8.2	0.2	0.08	0.1
10/10/2018	0	45.2	0.6	0.62	0.14	12.13	0.2	0.05	0.08
17/10/2018	59	107.1	1.3	6.41	0.54	29.91	0.6	9.3	0.83
24/10/2018	0	33.46	0.4	0.23	0.22	6.41	0.1	0.12	0.24
31/10/2018	0	136.61	1.7	2.32	0.17	54.62	1	2.74	0.58
14/11/2018	0	109.5	1.4	0.43	0.18	43.05	0.8	0.81	0.23
21/11/2018	6	24.87	0.3	0.81	0.36	39.16	0.7	0.76	0.16
10/12/2018	7	50.7	0.6	1.13	0.29	52.74	1	7.29	0.53
20/02/2019	3.2	87.07	1.1	1.49	0.21	78.84	1.5	2.37	0.36
22/02/2019	22	58.84	0.7	1.77	0.36	77.37	1.4	2.26	0.36
25/02/2019	0	68.74	0.8	1.19	0.16	99.28	1.8	1.96	0.31
07/03/2019	0	63.66	0.8	3.03	0.38	51.47	0.9	3.22	0.38
08/03/2019	0	96.24	1.2	2	0.29	59.58	1.1	3.33	0.39
21/03/2019	3.2	46.96	0.6	1.52	0.25	63.84	1.2	3.28	0.38
27/03/2019	3.4	49.08	0.6	1.77	0.3	77.71	1.4	3.01	0.35
04/04/2019	12.1	33.27	0.4	1.99	0.32	34.15	0.6	0.67	0.21
11/04/2019	2	35.84	0.4	2.52	0.22	29.47	0.5	0.7	0.29
03/05/2019	6	34.96	0.4	0.68	0.18	19.43	0.4	0.32	0.18
Means	6.77	60.54	0.8	1.67	0.26	46.52	0.9	2.35	0.33

[*] P, precipitation; *CSS*, concentration of suspended sediments; *QSS*, solid discharge in suspension; Q, flow

sediment transport. According to Larsen (2019), the soil cover can retain the sediment in the catchment area, preventing it from reaching the stream bed. The preservation of vegetation filter strips tended to increase the infiltration rate and reduce peak flows and floods.

This study provides useful information for future planning and management of natural resources and provides support in implementing strategies to mitigate the effects of increased soil loss in the region. In sub-basins that present similar conditions, the results of this study can be used to predict the hydrological behavior and sediment loads of data from data-scarce watersheds. In addition, this study may support future studies of ecological impacts in the Gurguéia and Parnaíba River basins, mainly in improving the methodological approach.

Conclusion

A quantitative assessment of soil erosion from CMSB using the USLE equation in the GIS environment

effectively provided a set of different spatial management approaches to estimate erosion in the sub-basin. The average annual loss of soil predicted by the USLE was 0–1 t ha^{-1}, being validated with the soil loss measured through the rain simulator.

The low transport of suspended sediments in CMSB is due to the existence of preserved sites. About 99% of the sub-basin had a low degree of erosion. The high degree of soil loss was attributed to the cliffs and the development of agricultural activities leaving the soil uncovered.

With the use of USLE combined with the GIS environment, it was possible to generate a map where it was possible to identify the areas most susceptible to erosion, facilitating the choice of appropriate conservation practices for the management of CMSB.

The USLE-SIG association was valid, but the erosion modeling in an area where there were eroded natural escarpments must be treated separately in the parameterization.

It is worth noting that the escarpments eroded at the edges of plateaus and plateaus, common and naturally

occurring in productive cerrado areas, limited the applicability of erosion models based on USLE when applied spatially. These interfered when determining the contribution or effective influence of the parameters related to slope and ramp length, limiting the modeling and tending to overestimate and generate erosion peaks outside the average representativeness of the area. In these bands of abrupt topography change, it was necessary to carefully parameterize the slope and ramp length factors of the USLE or even to exclude these bands.

References

Aghsaei, H., Dinan, N. M., Moridi, A., Asadolahi, Z., Delavar, M., Fohrer, N., & Wagner, P. D. (2020). Effects of dynamic land use/land cover change on water resources and sediment yield in the Anzali wetland catchment, Gilan, Iran. *Science of the Total Environment, 712*, 136449.

Alewell, C., Borelli, P., Meusburger, K., & Panagos, P. (2019). Using the USLE: chances, challenges and limitations of soil erosion modelling. *International Soil and Water Conservation Research, 7*(3), 203–225.

Ali, S. A., & Hagos, H. (2016). Estimation of soil erosion using USLE and GIS in Awassa Catchment, Rift valley, Central Ethiopia. *Geoderma Regional, 7*(2), 159–166.

Alves Sobrinho, T., Gómez-Macpherson, H., & Gómez, J. A. (2008). A portable integrated rainfall and overland flow simulator. *Soil Use and Management, 24*(2), 163–170.

Andrade Júnior, A. S., Alves, B. E., Cezar Barros, A. H., Oliveira Da Silva, C., & Nascimento Gomes, A. A. (2004). Classificação climática e regionalização do semi-árido do Estado do Piauí sob cenários pluviométricos distintos. *Revista Ciência Agronômica, 36*(2), 143–151.

Arnold, J. (1994). SWAT-soil and water assessment tool.

Back, A. J. (2006). Medidas de vazão com molinete hidrométrico e coleta de sedimentos em suspensão. *Boletim Técnico, 130*, 58. Florianópolis: EPAGRI (in Portuguese).

Batista, P. V. G., Silva, M. L. N., Silva, B. P. C., Curi, N., Bueno, I. T., Júnior, F. W. A., Davies, J., & Quinton, J. (2017). Modelling spatially distributed soil losses and sediment yield in the upper Grande River Basin-Brazil. *Catena, 157*, 139–150.

Bertoni, J., & Lombardi Neto, F. (2005). *Conservação do Solo* (5ª Edição, p. 392). São Paulo: Ícone Editora.

Brady N. C., & Weil R. R. (2009). *Elementos da natureza e propriedades dos solos* (3 ed., p. 686). Porto Alegre: Bookman Editora.

Carvalho, N. O. (1994). *Hidrossedimentologia prática* (p. 372). Rio de Janeiro: CPRM - Companhia de Pesquisa em Recursos Minerais.

Carvalho, N. O., Júnior, N. P., Santos, P. M. C., & Lima, J. F. E. W. (2000). *Guia de Práticas sedimentométricas* (154p). Brasília – DF: ANEEL.

Corrêa, C. M. C., & Dedecek, R. A. (2009). Erosão real e estimada através da RUSLE em estradas de uso florestais, em condições de relevo plano a suave ondulado. *Floresta, PR, 39*(2), 381–391 abr./jun.

Edwards, T. K., & Glysson, G. D. (1999). *Field methods for measurement of fluvial sediment* (Book 3, Chapter C2, p. 97.). Techniques of Water-Resources Investigations of the U.S. Geological Survey (USGS). USGS: Reston.

El Jazouli, A., Barakat, A., Khellouk, R., Rais, J., & El Baghdadi, M. (2019). Remote sensing and GIS techniques for prediction of land use land cover change effects on soil erosion in the high basin of the Oum Er Rbia River (Morocco). *Remote Sensing Applications: Society and Environment, 13*, 361–374.

Fujihara, A. K. (2002). *Predição de erosão e capacidade de uso do solo numa microbacia do Oeste Paulista com suporte de geoprocessamento* (p. 136). Piracicaba: Dissertação (Mestrado) – Escola Superior de Agricultura Luíz de Queiroz, Universidade de São Paulo.

Ganasri, B. P., & Ramesh, H. (2016). Assessment of soil erosion by RUSLE model using remote sensing and GIS-a case study of Nethravathi Basin. *Geoscience Frontiers, 7*(6), 953–961.

García-Ruiz, J. M., Nadal-Romero, E., Lana-Renault, N., & Beguería, S. (2013). Erosion in Mediterranean landscapes: changes and future challenges. *Geomorphology, 198*, 20–36.

Gee, G. W., & Bauder, J. W. (1986). Particle size analysis. In Klute (Ed.), *Methods of soil analysis, Part A* (2nd ed., Vol. 9 nd, pp. 383–411). Madison: American Society of Agronomy.

Gessesse, B., Bewket, W., & Bräuning, A. (2015). Model-based characterization and monitoring of runoff and soil erosion in response to land use/land cover changes in the Modjo watershed, Ethiopia. *Land Degradation & Development, 26*(7), 711–724.

Guo, L., Brand, M., Sanders, B. F., Foufoula-Georgiou, E., & Stein, E. D. (2018). Tidal asymmetry and residual sediment transport in a short tidal basin under sea level rise. *Advances in Water Resources., 121*, 1–8.

Hao, F., Zhang, X., Wang, X., & Ouyang, W. (2012). Assessing the Relationship Between Landscape Patterns and Nonpoint-Source Pollution in the Danjiangkou Reservoir Basin in China 1. *JAWRA Journal of the American Water Resources Association, 48*(6), 1162–1177.

Júnior, A. A. C., Da Conceição, F. T., Fernandes, A. M., Junior, E. P. S., Lupinacci, C. M., & Moruzzi, R. B. (2019). Land use changes associated with the expansion of sugar cane crops and their influences on soil removal in a tropical watershed in São Paulo State (Brazil). *Catena, 172*, 313–323.

Kok, K., & Kim, J. C. (2019). Identification of vulnerable regions to soil loss under the dynamic saturation process. *Science of the Total Environment, 659*, 1209–1223.

Larsen, L. G. (2019). Multiscale flow-vegetation-sediment feedbacks in low-gradient landscapes. *Geomorphology., 334*, 165–193.

Lazzari, M., Gioia, D., Piccarreta, M., Danese, M., & Lanorte, A. (2015). Sediment yield and erosion rate estimation in the

mountain catchments of the Camastra artificial reservoir (Southern Italy): a comparison between different empirical methods. *Catena, 127*, 323–339.

Mehri, A., Salmanmahiny, A., Tabrizi, A. R. M., Mirkarimi, S. H., & Sadoddin, A. (2018). Investigation of likely effects of land use planning on reduction of soil erosion rate in river basins: Case study of the Gharesoo River Basin. *Catena, 167*, 116–129.

Merten, G. H., & Poleto, C. (2006). *Qualidade dos Sedimentos* (397p). Porto Alegre, RS: Associação Brasileira de Recursos Hídricos – ABRH.

Minella, J. P. G., De, W., & Merten, G. H. (2014). Establishing a sediment budget for a small agricultural catchment in southern Brazil, to support the development of effective sediment management strategies. *Journal of Hydrology., 519*, 2189–2201.

Morais, R. C. S., & Sales, M. C. L. (2017). Estimativa do Potencial Natural de Erosão dos Solos da Bacia Hidrográfica do Alto Gurguéia, Piauí-Brasil, com uso de Sistema de Informação Geográfica/Estimation of the natural soil erosion potential of the Upper Gurguéia Basin, Piauí-Brazil (...). *Caderno de Geografia, 27*(1), 84–105.

Nunes, A. N., De Almeida, A. C., & Coelho, C. O. (2011). Impacts of land use and cover type on runoff and soil erosion in a marginal area of Portugal. *Applied Geography, 31*(2), 687–699.

Ochoa, P. A., Fries, A., Mejía, D., Burneo, J. I., Ruíz-Sinoga, J. D., & Cerdà, A. (2016). Effects of climate, land cover and topography on soil erosion risk in a semiarid basin of the Andes. *Catena, 140*, 31–42.

Okin, G. S., Heras, M. M. D. L., Saco, P. M., Throop, H. L., Vivoni, E. R., Parsons, A. J., et al. (2015). Connectivity in dryland landscapes: shifting concepts of spatial interactions. *Frontiers in Ecology and the Environment, 13*(1), 20–27.

Panachuki, E., Bertol, I., Alves Sobrinho, T., Oliveira, P. T. S. D., & Rodrigues, D. B. B. (2011). Perdas de solo e de água e infiltração de água em Latossolo Vermelho sob sistemas de manejo. *Revista Brasileira de Ciência do solo, 35*(5), 1777–1786.

Panagos, P., Borrelli, P., Meusburger, K., Alewell, C., Lugato, E., & Montanarella, L. (2015). Estimating the soil erosion cover-management factor at the European scale. *Land use policy, 48*, 38–50.

Pantano, G., Grosseli, G. M., Mozeto, A. A., & Fadini, P. S. (2016). Sustentabilidade no uso do fósforo: uma questão de segurança hídrica e alimentar. *Quimica Nova, 39*(6), 732–740.

Pham, T. G., Degener, J., & Kappas, M. (2018). Integrated universal soil loss equation (usle) and geographical information system (GIS) for soil erosion estimation in a sap basin: Central Vietnam. *International Soil and Water Conservation Research, 6*(2), 99–110.

Rey, F. (2003). Influence of vegetation distribution on sediment yield in forested marly gullies. *Catena, 50*(2-4), 549–562.

Saco, P. M., Rodríguez, J. F., Moreno-de las Heras, M., Keesstra, S., Azadi, S., Sandi, S., et al. (2020). Using hydrological connectivity to detect transitions and degradation thresholds: applications to dryland systems. *Catena, 186*, 104354.

Shivhare, N., Rahul, A. K., Omar, P. J., Chauhan, M. S., Gaur, S., Dikshit, P. K. S., & Dwivedi, S. B. (2018). Identification of critical soil erosion prone areas and prioritization of micro-watersheds using geoinformatics techniques. *Ecological Engineering, 121*, 26–34.

Silva, Y. J. A. B., Cantalice, J. R. B., Singh, V. P., Nascimento, C. W. A., Piscoya, V. C., & Guerra, S. M. S. (2015). Trace element fluxes in sediments of an environmentally impacted river. *Environmental Science and Pollution Research, 22*(19), 14755–14766. https://doi.org/10.1007/s11356-015-4670-9.

Silva, Y. J. A. B., do Nascimento, C. W. A., da Silva, Y. J. A. B., Amorim, F. F., Cantalice, J. R. B., Singh, V. P., & Collins, A. L. (2018). Bed and suspendedsediment-associated rare earth element concentrations and fluxes ina polluted Brazilian river system. *Environmental Science and Pollution Research, 25*(34), 34426–34437.

Singh, G., & Panda, R. K. (2017). Grid-cell based assessment of soil erosion potential for identification of critical erosion prone areas using USLE, GIS and remote sensing: A case study in the Kapgari watershed, India. *International Soil and Water Conservation Research, 5*(3), 202–211.

Teixeira, P. C., Donagemma, G. K., Fontana, A., & Teixeira, W. G. (2017). *Manual de métodos de análise de solo*. Brasília: Embrapa Solos.

Tian, P., Lu, H., Feng, W., Guan, Y., & Xue, Y. (2020). Large decrease in streamflow and sediment load of Qinghai–Tibetan Plateau driven by future climate change: a case study in Lhasa River Basin. *Catena, 187*, 104340.

UNITED STATES GEOLOGICAL SURVEY (USGS). (1973). *Techniques of Water Resources Investigations*. Washington. https://www.usgs.gov/.

Wischmeier, W. H. (1978). Use and misuse of the universal soil loss equation. *Journal of Soil and Water Conservation, 31*, 5–9.

Yuan, K. N. (1963). Studies on the organo-mineral complex in soil I. The oxidation stability of humus from different organo-mineral complexes in soil. *Acta Pedol Sin, 3*, 286–293.

Zhou, M., Deng, J., Lin, Y., Belete, M., Wang, K., Comber, A., & Gan, M. (2019). Identifying the effects of land use change on sediment export: integrating sediment source and sediment delivery in the Qiantang River Basin, China. *Science of the Total Environment, 686*, 38–49.

Springer